# Polyesters with Built-in Threshold Temperature and Deformation Sensors

Maki Kinami, Brent R. Crenshaw, and Christoph Weder*

*Department of Macromolecular Science and Engineering, Case Western Reserve University, 2100 Adelbert Road, Cleveland, Ohio 44106-7202*

*Received September 30, 2005. Revised Manuscript Received December 6, 2005*

The preparation and characterization of blends of polyesters and excimer-forming, photoluminescent 1,4-bis-(α-cyano-styryl)-benzenes, which function as built-in deformation or threshold temperature sensors, are described. Binary blends of poly(ethylene terephthalate) (PET) or poly(ethylene terephthalate glycol) (PETG) and small amounts (0.2−2% w/w) of a series of sensor dyes were prepared by melt-processing. The phase behavior of these materials can be controlled via the composition, the nature of solubility-controlling substituents attached to the dyes, and the processing protocol. Subjecting appropriately processed samples to either temperatures above their glass transition or mechanical deformation can significantly change the extent of molecular aggregation of the photoluminescent guest molecules, which in turn leads to a variation of the contributions of monomer and excimer emission. Since the emission maxima associated with these transitions can differ by as much as 138 nm, this change can readily be detected by spectroscopic means and in many cases even by the unassisted eye.

## Introduction

Förster and Kasper discovered 50 years ago that a pair of identical photoluminescent (PL) molecules could form an excimer, i.e., a complex between a molecule in an electronically excited state and a molecule of the same species in its ground state.[1] The bound excimer has a lower potential energy than that of the separated components (i.e., a molecule in its first electronically excited state and a molecule in its ground state) and therefore excimers emit at higher wavelengths than the monomer[2] species from which they are constituted. It has long been recognized that the formation of excimers in polymerics comprising a fluorescent probe can be used to extract structural information on the molecular (e.g., conformation and dynamics of macromolecules in solution[3]) as well as supramolecular level (e.g., miscibility of polymer blends,[4] morphology,[5] and distribution of dopant-site sizes[6]). The spectroscopic detection of excimers was also employed to sense the aggregation of guest molecules such as pyrene[7] in polystyrene,[8] polyethylene,[9] and other host polymers. In solution, excimer formation is frequently a dynamic, diffusion-controlled process.[10] By contrast, diffusion of the dye molecules in solid polymers is usually slow compared to the lifetime of the excited states, and excimers often predominantly arise from preformed aggregates.[11]

We recently demonstrated the possibility to exploit excimer-forming dyes for the design of polymers with "built-in" deformation sensors.[12,13] These materials are based on the integration of small amounts of the PL dyes into ductile host polymers and rely on the initial formation of nanoscale aggregates of the sensor molecules in the polymer matrix. In the example of linear low-density polyethylene we showed that apparently very small dye aggregates can be produced by guest-diffusion[12] and also by quenching and subsequently annealing melt-processed blends.[13] The approach exploits that mechanical deformation of these nanocomposites leads to shear-induced mixing,[14] which transforms the nanophase-separated systems into molecular mixtures, concomitant with a pronounced shift from excimer- to monomer-dominated emission. The inverse mechanism, i.e., the phase separation of initially molecularly mixed blends of excimer-forming dyes and glassy host polymers,[15] or as we show here semicrystalline host polymers with a glass transition in a temperature regime of interest, represents another versatile

(1) (a) Förster, T.; Kasper, K. *Z. Phys. Chem. NF* **1954**, *1*, 275. (b) Förster, T.; Kasper, K. *Z. Elektrochem. Angew. Phys. Chem.* **1955**, *59*, 976.
(2) In line with the common terminology, the term "monomer" is used here to describe emission from single-molecule excited states, as opposed to excimers.
(3) See for example: (a) Fitzgibbon, P. D.; Frank, C. W. *Macromolecules* **1981**, *14*, 1650. (b) Turro, N. J.; Arora, K. S. *Polymer* **1986**, *27*, 783. (c) Oyama, H. T.; Tang, W. T.; Frank, C. W. *Macromolecules* **1987**, *20*, 474. (d) Wang, Y. C.; Morawetz, H. *Macromolecules* **1989**, *22*, 164.
(4) See for example: (a) Semerak, S. N.; Frank, C. W. *Macromolecules* **1981**, *14*, 443. (b) Gashgari, M. A.; Frank, C. W. *Macromolecules* **1981**, *14*, 1558. (c) Gelles, R.; Frank, C. W. *Macromolecules* **1982**, *15*, 1486. (d) Semerak, S. N.; Frank, C. W. *Macromolecules* **1984**, *17*, 1148.
(5) See for example: (a) Zimerman, O. E.; Weiss, R. G. *J. Phys. Chem. A* **1998**, *102*, 5364. (b) Vigil, M. R.; Bravo, J.; Baselga, J.; Yamaki, S. B.; Atvars, T. D. Z. *Curr. Org. Chem.* **2003**, *7*, 197.
(6) See for example: Naciri, J.; Weiss, R. G. *Macromolecules* **1989**, *22*, 3928.
(7) Birks, J. B. *Rep. Prog. Phys.* **1975**, *38*, 903.
(8) Johnson, G. E. *Macromolecules* **1980**, *13*, 839.
(9) Szadkowska-Nicze, M.; Wolszczak, M.; Kroh, J.; Mayer, J. *J. Photochem. Photobiol. A: Chem.* **1993**, *75*, 125.
(10) (a) Döller, E.; Förster, T. *Z. Phys. Chem.* **1962**, *34*, 132. (b) Birks, J. B.; Dyson, D. J.; Munro, I. H. *Prog. R. Soc.* **1963**, *275 (Ser. A)*, 575.
(11) Spies, C.; Gehrke, R. *J. Phys. Chem.* **2002**, *106*, 5348.
(12) Löwe, C.; Weder, C. *Adv. Mater.* **2002**, *14*, 1625.
(13) Crenshaw, B. R.; Weder, C. *Chem. Mater.* **2003**, *15*, 4717.
(14) Trabesinger, W.; Renn, A.; Hecht, B.; Wild, U. P.; Montali, A.; Smith, P.; Weder, C. *J. Phys. Chem. B.* **2000**, *104*, 5221.
(15) Crenshaw, B. R.; Weder, C. *Adv. Mater.* **2005**, *17*, 1471.

10.1021/cm052186c CCC: $33.50 
Published on Web 01/21/2006

**Scheme 1. Synthesis of the Photoluminescent Dyes Employed**

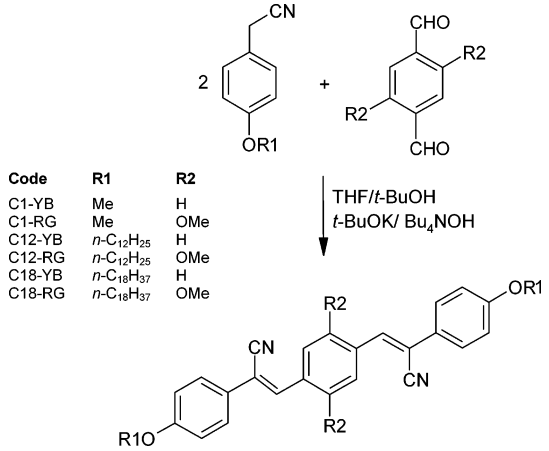


sensing mechanism, which is useful for the fabrication of threshold temperature sensors or time−temperature indicators.[16] In this case, the sensing scheme relies on kinetically trapping thermodynamically unstable molecular mixtures of the sensor dyes in the glassy amorphous phase of the polymer, for example, by melt-processing and rapid quenching below the glass transition temperature ($T_g$).[15] Subjecting these materials to temperatures above $T_g$ leads to permanent and pronounced changes of their PL emission spectra, as a result of phase separation and excimer formation.

A plethora of excimer-forming dyes,[17] including perylenes,[6] bis(benzoxazolyl)stilbenes,[18] and cyano-substituted oligo(*p*-phenylene vinylene) derivatives (cyano-OPVs, Scheme 1)[19−23] is suitable for these sensing schemes. We found that cyano-OPVs are particularly useful since they often exhibit a strong tendency toward excimer formation and display remarkably large differences (up to 140 nm) between the emission maxima of molecular solutions and aggregates.[23] Further, their optical characteristics and solubility in different host polymers are readily controlled via the nature of substituents attached to the aromatic rings, and their good thermal stability allows the incorporation into polymers by conventional melt-processing techniques.[23]

The previous work on polymers with built-in deformation sensors in our group[12,13] and elsewhere[18] was limited to semicrystalline polyolefins as host materials. On the other hand, our previous experiments on polymers with built-in threshold temperature sensors exclusively relied on glassy amorphous materials: poly(methyl methacrylate) and poly(bisphenol A carbonate).[15] To answer the question if the sensing schemes can be broadly exploited, we here present an investigation of binary blends of various new cyano-OPVs and poly(ethylene terephthalate) (PET) as an example of a polar, semicrystalline polymer and poly(ethylene terephthalate glycol) (PETG) as an example of a ductile, amorphous polymer. Our results unequivocally demonstrate that both threshold temperature, as well as deformation sensors can be realized on the basis of these materials platforms, if adequate processing schemes are employed.

## Experimental Section

**Materials.** 1,4-Bis(α-cyano-4-methoxystyryl)benzene (**C1-YB**),[23] 1,4-bis(α-cyano-4-methoxystyryl)-2,5-dimethoxybenzene (**C1-RG**),[23] and 2,5-dimethoxy terephthaldicarboxyaldehyde[24] were prepared as described before. All solvents employed were of analytical grade. Spectroscopy-grade chloroform (stabilized with 0.8% v/v ethanol) was used for all spectroscopic experiments. All chemicals were of highest commercial quality and were used as-received. A commercial-grade PET received from TOYOBO ($T_g$ = 78 °C; [$\eta$] = 0.63 dL/g measured at 30 °C in phenol/1,1,2,2,-tetrachloroethane 6/4 w/w,) and a commercially available PETG from Eastman Chemical Company (Eastman 6763, $T_g$ = 78 °C) were used as host polymers.

**General Methods.** $^1$H NMR spectral data are expressed in ppm relative to internal TMS and were obtained in $CDCl_3$ on a Varian XL (300 MHz) spectrometer. Differential scanning calorimetry (DSC) experiments were conducted under a $N_2$ atmosphere on a Perkin-Elmer DSC Pyris 1 at heating and cooling rates of 10 °C/min.

**Synthesis of (4-Dodecyloxyphenyl)acetonitrile.** A suspension of $K_2CO_3$ (4.05 g, 29.2 mmol) in dimethylformamide (15 mL) was purged with Ar for 15 min and heated to 80 °C, and 4-hydroxyphenylacetonitrile (1.47 g, 11.0 mmol) was added. After stirring at 80 °C for 10 min, 1-bromododecane (3.54 g, 14.2 mmol) was slowly added and the suspension was stirred at 80 °C under Ar for another 4 h. After this time a pale yellow precipitate had formed. The reaction was terminated by pouring the suspension into ice−water (150 mL) and $CHCl_3$ (50 mL) was added to dissolve the precipitate. The organic layer was separated off and the aqueous phase was extracted with $CHCl_3$ (3 × 50 mL). The combined organic layers were washed with $H_2O$ and saturated aqueous NaCl. The organic phase was dried with $MgSO_4$ and filtered, and the solvent was evaporated in vacuo to yield a pale yellow powder (3.30 g). Recrystallization from EtOH (50 mL) afforded (4-dodecyloxyphenyl)acetonitrile in the form of white crystals (2.56 g, 77%). $^1$H NMR: $\delta$ = 7.23 Hz (d, 2 H, ArH), 6.89 Hz (d, 2 H, ArH), 3.95 Hz (t, 2 H, $CH_2$−O), 3.69 Hz (s, 2 H, $CH_2$−CN), 1.7−1.9 Hz (m, 2 H, $CH_2$), 1.5−1.2 Hz (m, 18 H, 9 × $CH_2$), 0.89 Hz (t, 3 H, $CH_3$).

**Synthesis of 1,4-Bis(α-cyano-4-dodecyloxystyryl)-2,5-dimethoxybenzene (C12-RG).** 2,5-Dimethoxyterephthaldehyde (146 mg, 0.75 mmol) and (4-dodecyloxyphenyl)acetonitrile (500 mg, 1.66 mmol) were dissolved at 70 °C in a mixture of *t*-BuOH (11 mL) and THF (5 mL). *t*-BuOK (0.11 mL of a 1 M solution in THF, 0.11 mmol) and *n*-$Bu_4NOH$ (1 mL of a 1 M solution in MeOH, 1 mmol) were

(16) See for example: (a) Allegra, J. E.; Brennan, J.; Lanier, V.; Lavery, R.; MacKenzie, B. *Acad. Emerg. Med.* **1999**, *6*, 1098. (b) Shimoni, E.; Anderson, E. M.; Labuza, T. P. *J. Food. Sci.* **2001**, *66*, 1337.
(17) Birks, J. B. *Rep. Prog. Phys.* **1975**, *38*, 903.
(18) Pucci, A.; Bertoldo, M.; Bronco, S. *Macromol. Rapid. Commun.* **2005**, *26*, 1043.
(19) (a) Gill, R. E.; van Hutten, P. F.; Meetsma, A.; Hadziioannou, G. *Chem. Mater.* **1996**, *8*, 1341. (b) van Hutten, P. F.; Krasnikov, V. V.; Brouwer, H.-J.; Hadziioannou, G. *Chem. Phys.* **1999**, *241*, 139.
(20) (a) Döttinger, S. E.; Hohloch, M.; Hohnholz, D.; Segura, J. L.; Steinhuber, E.; Hanack, M. *Synth. Met.* **1997**, *84*, 267. (b) Hohloch, M.; Maichle-Mössmer, C.; Hanack, M. *Chem. Mater.* **1998**, *10*, 1327. (c) Oelkrug, D.; Tompert, A.; Gierschner, J.; Egelhaaf, H.-J.; Hanack, M.; Hohloch, M.; Steinhuber, E. *J. Phys. Chem. B* **1998**, *102*, 1902. (d) Martinez-Ruiz, P.; Behnisch, B.; Schweikart, K.-H.; Hanack, M.; Lüer, L.; Oelkrug, D. *Chem. Eur. J.* **2000**, *6*, 1294. (e) Freudenmann, R.; Behnisch, V.; Hanack, M. *J. Mater Chem.* **2001**, *11*, 1618.
(21) Henari, F. Z.; Manaa, H.; Kretsch, K. P.; Blau, W. J.; Rost, H.; Pfeiffer, S.; Teuschel, A.; Tillmann, H.; Hörhold, H. H. *Chem. Phys. Lett.* **1999**, *307*, 163.
(22) de Souza, M. M.; Rumbles, G.; Gould, I. R.; Amer, H.; Samuel, I. D. W.; Moratti, S. C.; Holmes, A. B. *Synth. Met.* **2000**, *111−112*, 539.
(23) (a) Löwe, C.; Weder, C. *Synthesis* **2002**, *9*, 1185. (b) Crenshaw, B.; Smith, K.; Weder, C. *Polym. Prepr. (Am. Chem. Soc., Div. Polym. Chem.)* **2005**, *46* (1), 532. (c) Crenshaw, B.; Burnworth, M.; Kunzelman, J.; Mendez, J.; Smith, K.; Weder, C. *Polym. Prepr. (Am. Chem. Soc., Div. Polym. Chem.)* **2005**, *46* (1), 506.
(24) Irngartinger, H.; Herpich, R. *Eur. J. Org. Chem.* **1998**, *365*, 628.

added quickly and an orange precipitate started to form immediately. The mixture was stirred for 15 min at 70 °C, cooled to RT, and poured into acidified methanol (50 mL containing 1 drop of concentrated acetic acid). The resulting precipitate was filtered off, excessively washed with MeOH, and dried in vacuo at 50 °C to yield **C12-RG** (515 mg, 90%) in the form of orange crystals. DSC: K 93 °C (2.64 J/g), LC 112 °C (3.38 J/g), I 166 °C (52.4 J/g). $^1$H NMR: $\delta$ = 7.90 Hz (2 × s, 2 × 2 H, ArH + CH═CCN), 7.67 Hz (d, 4 H, ArH), 6.99 Hz (d, 4 H, ArH), 4.02 Hz (t, 4 H, O−$CH_2$), 3.97 Hz (s, 6 H, O−$CH_3$), 1.8 Hz (m, 4 H, $CH_2$), 1.6−1.2 Hz (m, 36 H, 9 × $CH_2$), 0.90 Hz (t, 6 H, $CH_3$). Anal. Calcd for $C_{50}H_{68}O_4N_2$: C, 78.91; H, 9.01; N, 3.68; O, 8.41. Found: C, 78.16; H, 9.15; N, 3.61; O, 9.09.

**Synthesis of 1,4-Bis(α-cyano-4-dodecyloxystyryl)benzene (C12-YB).** Terephthaldehyde (101 mg, 0.75 mmol) and (4-dodecyloxyphenyl)acetonitrile (500 mg, 1.66 mmol) were dissolved at 70 °C in a mixture of *t*-BuOH (11 mL) and THF (8 mL). *t*-BuOK (0.11 mL of a 1 M solution in THF, 0.11 mmol) and *n*-$Bu_4NOH$ (1 mL of a 1 M solution in MeOH, 1 mmol) were added quickly at 70 °C, and a yellow precipitate started to form immediately. The mixture was stirred for 15 min at 70 °C, cooled to RT, and poured into acidified methanol (50 mL containing 1 drop of concentrated acetic acid). The resulting precipitate was filtered off, excessively washed with MeOH, and dried in vacuo at 50 °C to yield **C12-YB** (446 mg, 84%) in the form of a yellow powder. DSC: K 117 °C (3.3 J/g), LC 149 °C (87.6 J/g), I 194 °C (19.4 J/g). $^1$H NMR: $\delta$ = 7.96 Hz (s, 4 H, ArH), 7.64 Hz (d, 4 H, ArH), $\delta$ = 7.44 Hz (s, 2 H, CH═CCN), 7.97 Hz (d, 4 H, ArH), 4.02 Hz (t, 4 H, O−$CH_2$), 1.8 Hz (m, 4 H, $CH_2$), 1.5 Hz (m, 4H, $CH_2$), 1.4−1.2 Hz (m, 36 H, 9 × $CH_2$), 0.90 Hz (t, 6 H, $CH_3$). Anal. Calcd for $C_{48}H_{64}O_2N_2$: C, 82.24; H, 9.20; N, 4.00; O, 4.56. Found: C, 82.15; H, 9.48; N, 3.97; O, 4.95.

**Synthesis of (4-Octadecyloxyphenyl)acetonitrile.** A suspension of $K_2CO_3$ (4.05 g, 29.2 mmol) and dimethylformamide (15 mL) was purged with Ar for 15 min and heated to 80 °C, and 4-hydroxyphenylacetonitrile (1.47 g, 11.0 mmol) was added. After 10 min, 2-bromooctadecane (4.03 g, 12.1 mmol), which had been liquefied by warming to 30 °C in a water bath, was slowly added via a syringe, and the suspension was stirred at 100 °C under Ar for another 4 h. After this time, a pale yellow precipitate had formed. The reaction was terminated by pouring the suspension into ice−water (150 mL) and $CHCl_3$ (50 mL) was added to dissolve the precipitate. The organic layer was separated off and the aqueous phase was extracted with $CHCl_3$ (3 × 50 mL). The combined organic layers were washed with $H_2O$ and saturated aqueous NaCl. The organic phase was dried with $MgSO_4$ and filtered, and the solvent was evaporated in vacuo to yield a pale yellow powder (4.20 g). Recrystallization from EtOH (80 mL) afforded (4-octadecyloxyphenyl)acetonitrile in the form of pale yellow crystals (3.69 g, 87%). $^1$H NMR: $\delta$ = 7.22 Hz (d, 2 H, ArH), 6.89 Hz (d, 2 H, ArH), 3.95 Hz (t, 2 H, $CH_2$−O), 3.69 Hz (s, 2 H, $CH_2$−CN), 1.7−1.8 Hz (m, 2 H, $CH_2$), 1.5−1.2 Hz (m, 30 H, 15 × $CH_2$), 0.89 Hz (t, 3 H, $CH_3$).

**Synthesis of 1,4-Bis(α-cyano-4-octadecyloxystyryl)-2,5-dimethoxybenzene (C18-RG).** 2,5-Dimethoxyterephthaldehyde (115 mg, 0.59 mmol) and (4-octadecyloxyphenyl)acetonitrile (500 mg, 1.30 mmol) were dissolved at 80 °C in a mixture of *t*-BuOH (11 mL) and THF (7 mL). *t*-BuOK (0.09 mL of a 1 M solution in THF, 0.09 mmol) and *n*-$Bu_4NOH$ (1 mL of a 1 M solution in MeOH, 1 mmol) were added quickly and an orange precipitate started to form immediately. The mixture was stirred for 15 min at 80 °C, cooled to RT, and poured into acidified methanol (50 mL containing 1 drop of concentrated acetic acid). The resulting precipitate was filtered off, excessively washed with MeOH, and dried in vacuo at 50 °C to yield **C18-RG** (495 mg, 90%) in the form of orange crystals. DSC: K 117 °C (13.0 J/g), LC 142 °C (25.9 J/g), I 154 °C (48.8 J/g). $^1$H NMR: $\delta$ = 7.89 Hz (s, 2 H, CH═CCN), $\delta$ = 7.64 Hz (s, 2 H, ArH), 6.97 Hz (d, 4 H, ArH), 4.01 (t, 4 H, O−$CH_2$), 3.96 (s, 6 H, O−$CH_3$), 1.8 Hz (m, 4 H, $CH_2$), 1.6−1.2 Hz (m, 60 H, 15 × $CH_2$), 0.89 Hz (t, 6 H, $CH_3$). Anal. Calcd for $C_{62}H_{92}O_4N_2$: C, 80.12; H, 9.98; N, 3.01; O, 6.89. Found: C, 79.88; H, 10.20; N, 2.93; O, 7.10.

**Synthesis of 1,4-Bis(α-cyano-4-octadecyloxystyryl)benzene (C18-YB).** Terephthaldehyde (79 mg, 0.59 mmol) and (4-octadecyloxyphenyl)acetonitrile (500 mg, 1.30 mmol) were dissolved at 70 °C in a mixture of *t*-BuOH (11 mL) and THF (7 mL). *t*-BuOK (0.09 mL of a 1 M solution in THF, 0.09 mmol) and *n*-$Bu_4NOH$ (1 mL of a 1 M solution in MEOH, 1 mmol) were added quickly and a yellow precipitate started to form immediately. The mixture was stirred for 15 min at 70 °C, cooled to RT, and poured into acidified methanol (50 mL containing 1 drop of concentrated acetic acid). The precipitate was filtered off, excessively washed with MeOH, and dried in vacuo at 50 °C to yield **C18-YB** (446 mg, 87%) in the form of a yellow powder. DSC: K 106 °C (10.7 J/g), LC1 114 °C (19.9 J/g), LC2 142 °C (93.1 J/g), I 179 °C (14.4 J/g). $^1$H NMR: $\delta$ = 7.96 Hz (s, 4 H, ArH), 7.63 Hz (d, 4 H, ArH), $\delta$ = 7.44 Hz (s, 2 H, CH═CCN), 6.98 Hz (d, 4 H, ArH), 4.02 Hz (t, 4 H, O−$CH_2$), 1.8 Hz (m, 4 H, $CH_2$), 1.6−1.2 Hz (m, 60 H, 15 × $CH_2$), 0.88 Hz (t, 6 H, $CH_3$). Anal. Calcd for $C_{60}H_{88}O_2N_2$: C, 82.89; H, 10.20; N, 3.22; O, 3.68. Found: C, 82.88; H, 10.53; N, 3.18; O, 3.75.

**Film Preparation.** PET pellets were dried in vacuo at 130 °C for 24 h, and PETG pellets were dried in vacuo at 80 °C for at least 4 h prior to processing. Binary blends of PET and each dye were prepared by feeding the appropriate amount of dye (0.2−2% w/w with respect to the polymer) and 4.0 g of PET into a recycling, co-rotating twin-screw mini-extruder (DACA Instruments, Santa Barbara, CA), mixing for 3 min at 280 °C, and subsequent extrusion. In some cases, dye residues remained in the extruder and the dye concentration in the blend produced was lower than expected from the feed. The dye concentration was therefore in all cases measured by optical means (vide infra). Films were prepared by compression-molding the blends between two pieces of aluminum foil covered with Kapton films and using aluminum spacers in a Carver press at 280 °C for approximately 1 min. The samples were immediately quenched after removal from the press by immersion in an ice−water bath. The resulting blend films had a homogeneous thickness of ca. 200 $\mu$m. Films based on PETG and the dyes were produced in an identical manner, but the processing temperature was 250 °C and the typical film thickness was 100 $\mu$m.

**Analysis of Dye Concentration in Films.** The dye concentration of the blend films was determined by comparative UV−Vis absorption spectroscopy. In the case of PET blends, 10 mg of the quenched films was dissolved in 10.5 mL of a mixture of 1,4-dichlorobenzene/$CHCl_3$/$CF_3COOH$ (1/9/0.5 v/v/v) and the absorbance of the resulting solutions at $\lambda_{max}$ was compared with that of a standard solution of the neat dye in the same solvent mixture. PETG blends films were analyzed in the same manner, but the solvent was chlorobenzene/$CHCl_3$ (1/9 v/v).

**Optical Spectroscopy.** UV−Vis absorption spectra were obtained on a Perkin-Elmer Lambda 800. Steady-state PL spectra were acquired on a SPEX Fluorolog FL3-12 and a PTI C720. Spectra were collected under excitation at 435 nm (RG dyes) and 375 nm (YB dyes) with excitation and emission slits set to 1.8 and 2.5 nm, respectively. All spectra are corrected for the instrument throughput and the detector response. All PL experiments were conducted at room temperature and were measured on free-standing films with detection from the front of the films. Annealing experiments were

**Table 1. Optical Absorption and PL Emission Characteristics of the Photoluminescent Dyes Employed**

| dye | R1[a] | R2[a] | Abs. $\lambda_{max}$ solution[b] [nm] | PL $\lambda_{max}$ solution[b] [nm] | PL $\lambda_{max}$ solid[c] [nm] | PL $\lambda_{monomer}$ PET[d] [nm] | PL $\lambda_{excimer}$ PET[d] [nm] |
|---|---|---|---|---|---|---|---|
| **C1-YB** | Me | H | 389 | 461, 486 | 550 | 496 | *e* |
| **C1-RG** | Me | OMe | 365, 436 | 506, 538 | 644 | 548 | *e* |
| **C12-YB** | $C_{12}H_{25}$ | H | 395 | 464, 489 | 481, 507 | 496 | *e* |
| **C12-RG** | $C_{12}H_{25}$ | OMe | 371, 436 | 506, 538 | 618 | 548 | *e* |
| **C18-YB** | $C_{18}H_{37}$ | H | 394 | 465, 489 | 481, 507 | 496 | *e* |
| **C18-RG** | $C_{18}H_{37}$ | OMe | 371, 437 | 507, 538 | 644 | 546 | 637 |

[a] See Scheme 1 for chemical structures. [b] Measured in $CHCl_3$ with a dye concentration of ca. $2-2.5 \times 10^{-3}$ mol·L$^{-1}$. [c] Powder as-synthesized. [d] Measured on melt-processed PET blend films. The values slightly depended on the dye concentration ($\lambda \pm 2$ nm). [e] No excimer observed at dye concentrations of up to 1% w/w.

carried out by placing the film samples directly on either a Wagner & Munz WME hot shoe with temperature gradient or on a Gel Instrumente AG hotstage in connection with a TC2 temperature controller.

## Results and Discussion

**Synthesis and Properties of Sensor Dyes.** The excimer-forming dyes employed in this study are based on the cyano-OPV motif, which we employed before for deformation sensing in polyolefins[12,13] and temperature sensing in polyacrylates and polycarbonate[15] (Scheme 1). Initial experiments (vide infra) of the present study relied on the previously described 1,4-bis(α-cyano-4-methoxystyryl)benzene,[23] which on account of the substitution pattern (R1 = C1 hydrocarbon chain) and excimer/monomer fluorescence color (yellow/blue) we refer to as **C1-YB**, and 1,4-bis-(α-cyano-4-methoxystyryl)-2,5-dimethoxybenzene,[23] which due to its substitution pattern (R1 = **C1** hydrocarbon chain) and excimer/monomer fluorescence color (red/green) we refer to as **C1-RG.** Not surprisingly, however, both these dyes exhibit an undesirably high solubility in the polyesters studied here (vide infra), and hence, we opted to extend the length of the alkyl chain R1 (C12, C18) to reduce the dye's solubility in polar polymers. We therefore synthesized 1,4-bis(α-cyano-4-dodecyloxystyryl)benzene (**C12-YB**), 1,4-bis-(α-cyano-4-dodecyloxystyryl)-2,5-dimethoxybenzene (**C12-RG**), 1,4-bis(α-cyano-4-octadecyloxystyryl)benzene (**C18-YB**), and 1,4-bis(α-cyano-4-octadecyloxystyryl)-2,5-dimethoxybenzene (**C18-RG**) as new representatives of this family of cyano-OPVs (Scheme 1). These PL dyes were prepared in good yield through the Knoevenagel reaction of the corresponding (4-alkyloxyphenyl)acetonitriles with terephthaldehyde (YB series) or 2,5-dimethoxyterephthaldehyde (RG series) under standard conditions[25] (see Experimental Section for details). In $CHCl_3$ solution the new dyes display, as expected, essentially identical photophysical properties as their C1 homologues **C1-YB** and **C1-RG** and emit in the blue (YB series, $\lambda_{max} \approx 464$, 489 nm) and green (RG series, $\lambda_{max} \approx 506$, 538 nm) regime of the visible spectrum (Table 1, Figure 1, spectra for the C12 series are shown in the Supporting Information). In the case of **C12-RG** and **C18-RG** a significant bathochromic shift can be observed when comparing the PL emission spectra of dilute $CHCl_3$ solutions with those of the crystalline dyes ($\lambda_{max} \approx 618$ and 644 nm, respectively), which emit orange light (Table 1, Figure 1). This behavior is similar to the one of **C1-RG** and is indicative of excimer formation upon crystallization. By contrast, steady-state PL emission spectra do not reveal any appreciable excimer emission in the crystalline form of **C12-YB** and **C18-YB** (Table 1, Figure 1). In view of the fact that excimer formation is observed for **C1-YB**,[23] this result is at first somewhat surprising. However, it suggests that **C12-YB** and **C18-YB** adopt crystal structures (at least when crystallized from ethanol, as was done here), which do not allow for adequate molecular orbital overlap of adjacent chromophores to allow for adequate electronic interaction.

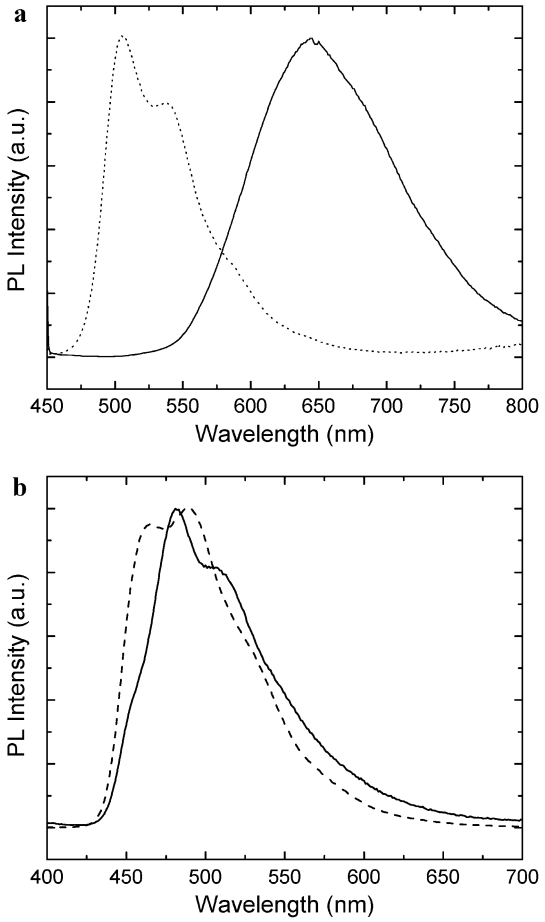


**Figure 1.** Normalized PL emission spectra of $CHCl_3$ solutions (dotted line) and "as-synthesized" crystals (solid line) of (a) **C18-RG** and (b) **C18-YB**.

The phase behavior of the new dyes was studied by means of differential scanning calorimetry (DSC) and polarized optical microscopy. All four new dyes display crystalline to liquid crystalline (LC) transitions in the regime of 93−117 °C. Different LC phases were observed for each dye before the isotropic melts were reached at 154−194 °C (see Experimental Section for details). Since the feature of liquid crys-

(25) Greenham, N. C.; Moratti, S. C.; Bradley, D. D. C.; Friend, R. H.; Holmes, A. B. *Nature* 1993, *365*, 628.

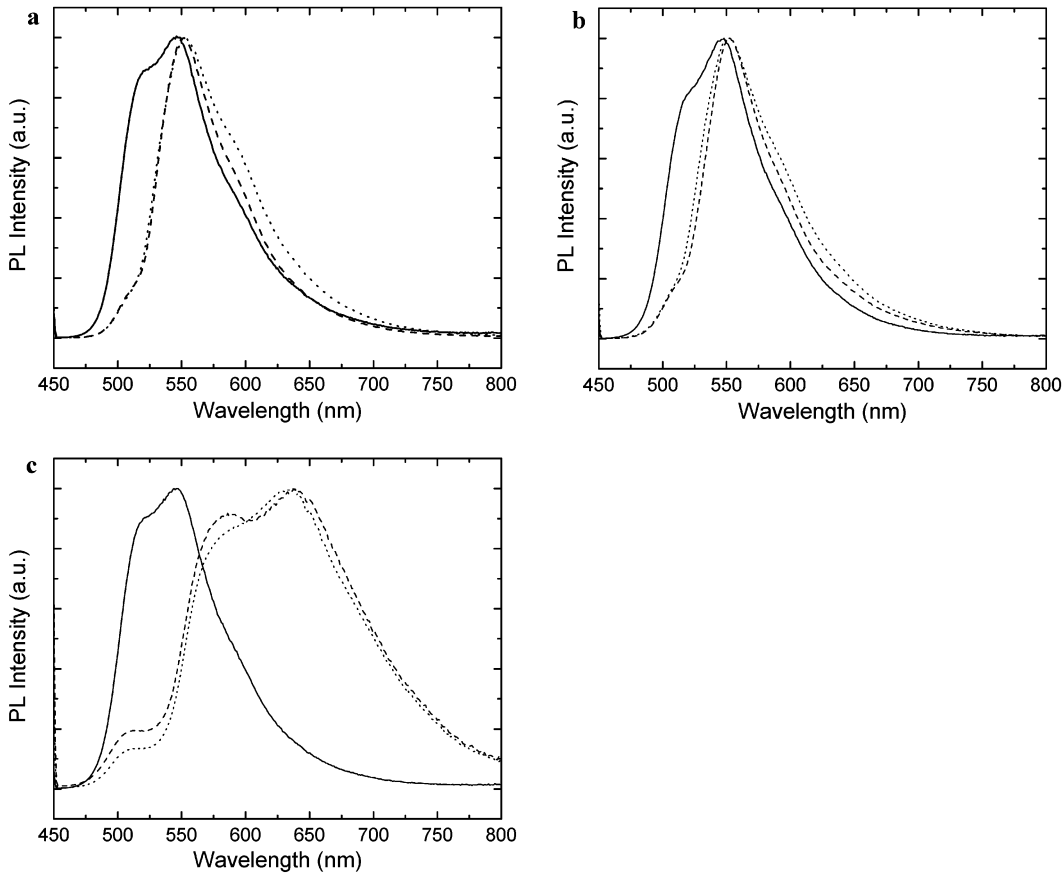


**Figure 2.** Normalized PL emission spectra of blend films based on PET and (a) 1% w/w **C1-RG**, (b) 1% w/w **C12-RG**, and (c) 0.9% w/w **C18-RG**. Shown are spectra of quenched films (solid line) and samples that were annealed for 2 h at 100 °C (dashed line) or 120 °C (dotted line).

tallinity is not of importance for the present work, we have not established the detailed nature of the various mesophases.

**Blends of Sensor Dyes with PET.** Binary blends of PET and 1% w/w (in the case of **C1-RG** and **C18-RG** between 0.2 and 2% w/w) of **C1-YB**, **C1-RG**, **C12-RG**, or **C18-RG** were prepared by melt-mixing the components at 280 °C in a co-rotating twin-screw mini-extruder (in-depth studies with **C12-YB** and **C18-YB** were omitted since they did not display excimer emission in the crystalline solid state; control experiments with slowly cooled blends of PET and 2% w/w of these dyes also confirmed the absence of excimer formation in PET). The resulting blends were subsequently compression-molded at the same temperature to produce films of a thickness of 200 $\mu$m. The processing temperature was in all cases above the isotropic melting temperature of the dye. After processing, the film samples were rapidly quenched to 0 °C in order to kinetically trap the dye in a molecularly dissolved or dispersed fashion in the glassy amorphous fraction of the host polymer as well as to suppress crystallization of the PET. The dye concentration of the blend films was determined by comparative UV−Vis absorption spectroscopy with reference to solutions of the neat dye. Upon excitation with ultraviolet (UV) light quenched blend films comprising **C1-YB** fluoresced blue ($\lambda_{max} \approx 496$ nm), while quenched samples comprising dyes of the RG series displayed green fluorescence ($\lambda_{max} \approx 546$ nm). Their emission spectra displayed modest (∼10 nm) hypsochromic shifts and a redistribution of the intensity of the phonon bands when compared to those of $CHCl_3$ solutions of the dyes (presumably due to internal reabsorption, which arises from the overlap of the dyes' absorption band with the high-energy portion of the emission spectra[15]) but otherwise matched the latter well (Table 1, Figure 2). Thus, the data indicate that upon quenching the PET/dye blends rapidly from the melt; the dye molecules are, at least at the concentration investigated here, incorporated in the PET matrix in an apparently molecularly dispersed or dissolved fashion.

To obtain some insights into the phase transitions and morphology of the PET/dye blends, the thermal behavior of selected samples was studied using differential scanning calorimetry (DSC). First heating and cooling scans of freshly quenched films of neat PET and a binary blend of PET and 0.9% w/w **C18-RG** are shown as in Figure 3. As can be seen from Figure 3a, the neat PET displays a glass transition at 78 °C, a cold crystallization peak with maximum at 152 °C, and a melting temperature of 256 °C. From the literature value for the heat of fusion for a (hypothetical) perfectly crystalline PET $\Delta H_m°$ (30 cal/g)[26] and the experimentally determined heats of cold crystallization $\Delta H_c$ (33.7 J/g) and fusion $\Delta H_m$ (45.2 J/g), we estimate a crystallinity of ∼9% for the quenched PET film and ∼36% for samples that were heated to the melting point at a rate of 10 °/min. The DSC of a quenched blend of PET and 0.9% w/w **C18-RG** (Figure 3b) reveals that $T_g$ is slightly reduced (by about 2 K to 76

(26) (a) Wunderlich, B. *Macromolecular Physics*; Academic Press: New York, 1973; Vol. 1, p 389. (b) Sekelik, D. J.; Stepanov, E. V.; Nazarenko, S.; Schiraldi, D.; Hiltner, A.; Baer, E. *J. Polym. Sci., Part B: Polym. Phys.* **1999**, *37*, 847.

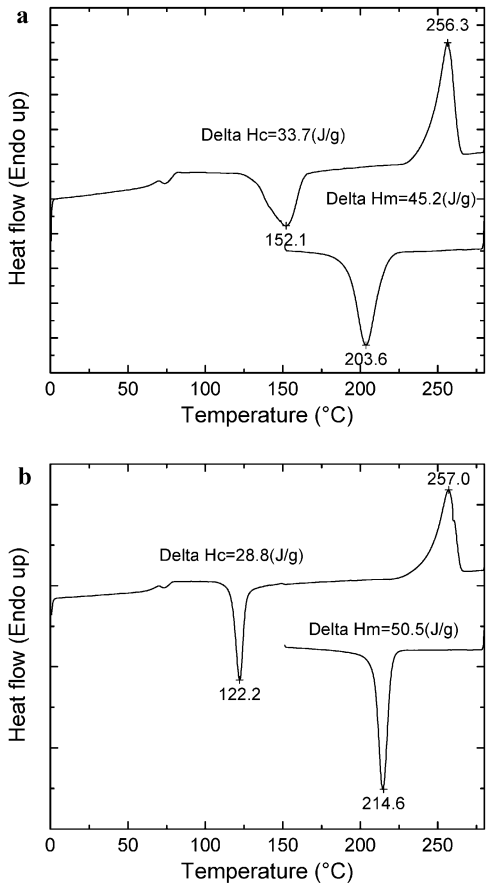


**Figure 3.** Differential scanning calorimetry (DSC) traces of quenched films of (a) neat PET and (b) a binary blend of PET and 0.9% w/w **C18-RG**. First heating (top curves) and cooling (bottom curves) scans were recorded at heating/cooling rates of 10 K/min.

°C). At the same time, the crystallization peaks observed for the blend in both heating and cooling scans are much sharper than those observed for the neat PET and their maxima are shifted to significantly lower temperature upon heating (122 instead of 152 °C) and higher temperature (215 instead of 204 °C) upon cooling. Further, the levels of crystallinity of the quenched blend (∼17%) and a blend sample that was heated to the melting point at a rate of 10 °C/min (∼40.2%) were found to be slightly higher than those for the corresponding samples of the neat PET. These data suggest that PET is significantly plasticized by even small amounts of **C18-RG**, an effect that is not uncommon and is routinely observed for a broad variety of additives that are incorporated in a molecularly dispersed fashion.[27]

In a series of annealing experiments all (initially quenched) PET/dye blends were annealed above their $T_g$ in order to study whether the dye molecules would aggregate if given adequate translational mobility. Initial screening experiments were carried out by placing film strips for 2 h on a hot stage that provided a spatial temperature gradient in the range of 90−150 °C. Additional annealing experiments were conducted at selected temperatures of between 90 and 140 °C. Interestingly, none of the blends comprising up to 1% w/w **C1-RG** (Figure 2a), 1% w/w **C12-RG** (Figure 2b), or 1% w/w **C1-YB** exhibited major optical changes upon annealing at these temperatures except for an increased opacity that is associated with the crystallization of the PET matrix upon annealing (vide infra). While the features associated with monomer emission typically narrowed and displayed a redistribution of the intensity of the phonon bands (see Figure 2a and 2b), the characteristic emission bands associated with excimer fluorescence remained almost completely absent in these annealed samples. These results suggest that, in the temperature/concentration space investigated here, the dye concentration in these blends is close to or below the solubility limit of the dyes. In light of the previously reported high solubility of **C1-YB** and **C1-RG** in polycarbonate,[15] this finding is, at least for these dyes, not a surprise. While blends of PET and **C1-RG**, **C12-RG**, or **C1-YB** can be expected to display phase separation at higher dye concentrations, we have omitted study of these compositions since high-solubility limits limit the optical contrast between quenched and annealed blends.[15] Gratifyingly, **C18-RG** displayed a lower solubility in PET than the other dyes investigated here. While the 0.2% w/w PET/**C18-RG** exclusively displayed monomer emission, the emission spectra of a 0.5% w/w PET/**C18-RG** blend film displayed a weak shoulder around 640 nm upon annealing at 100 °C (see Supporting Information for spectra). This change was much more pronounced in the case of 0.9% w/w **C18-RG** blend films that were annealed at a temperature of 90 °C or above. In this case, a dominant, unstructured red emission band centered at 637 nm developed upon annealing (Figure 2c). The red portion of the spectrum is characteristic of excimer emission and reflects phase separation and the formation of ground-state dye aggregates. The emission spectra of annealed 0.9% w/w PET/ **C18-RG** blend films display a shoulder in the range of 507−546 nm, which is characteristic of monomer emission and indicates that a fraction of dye molecules remains dissolved even after annealing. The fact that the excimer emission of 0.5% w/w PET/**C18-RG** blends disappears if the samples are annealed above 100 °C (see Supporting Information for spectra) suggests that the solubility of **C18-RG** in PET at 100 °C is close to 0.5% w/w, and one might expect a significant relative contribution of monomer emission (with respect to excimer) in 0.9% w/w **PET/C18-RG** films annealed at 100 °C. However, the fact that the emission spectra (Figure 2c) are dominated by excimer emission is consistent with internal re-absorption, caused by the high optical density of the samples investigated.

To further explore the influence of the annealing temperature, particularly with respect to the aggregation speed, we investigated the influence of the annealing parameters in greater detail. Figure 4 provides a graphical summary of some of these experiments with 0.9% w/w **PET/C18-RG** blend films and highlights a number of interesting features. Not surprisingly, the change from green monomer to orange excimer emission becomes faster as the annealing temperature is increased. While the transition takes hours at 90 °C (i.e., just above $T_g$), it is practically instantaneous at 140 °C. To probe kinetics of the aggregation process, we undertook a more detailed spectroscopic investigation. Figure 5a displays the spectra of 0.9% w/w PET/**C18-RG** blend films

(27) De Clerck, K.; Rahier, H.; Van Mele, B.; Kiekens, P. *J. Appl. Polym. Sci.* **2003**, *90*, 105.

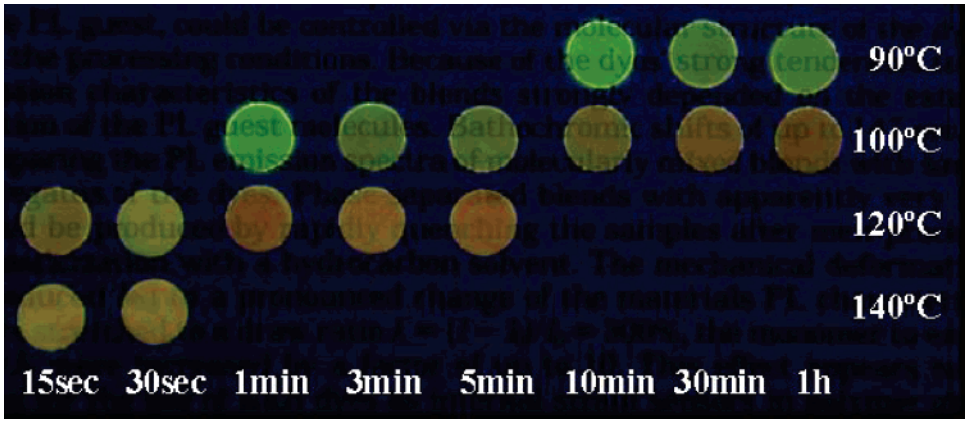


**Figure 4.** Pictures of initially quenched blends films of PET and 0.9% w/w **C18-RG** upon annealing for the time and at the temperature indicated. The samples are shown under illumination with UV light of a wavelength of 365 nm. Note that the different annealing protocols not only lead to different fluorescence colors but also different degrees of opacity.

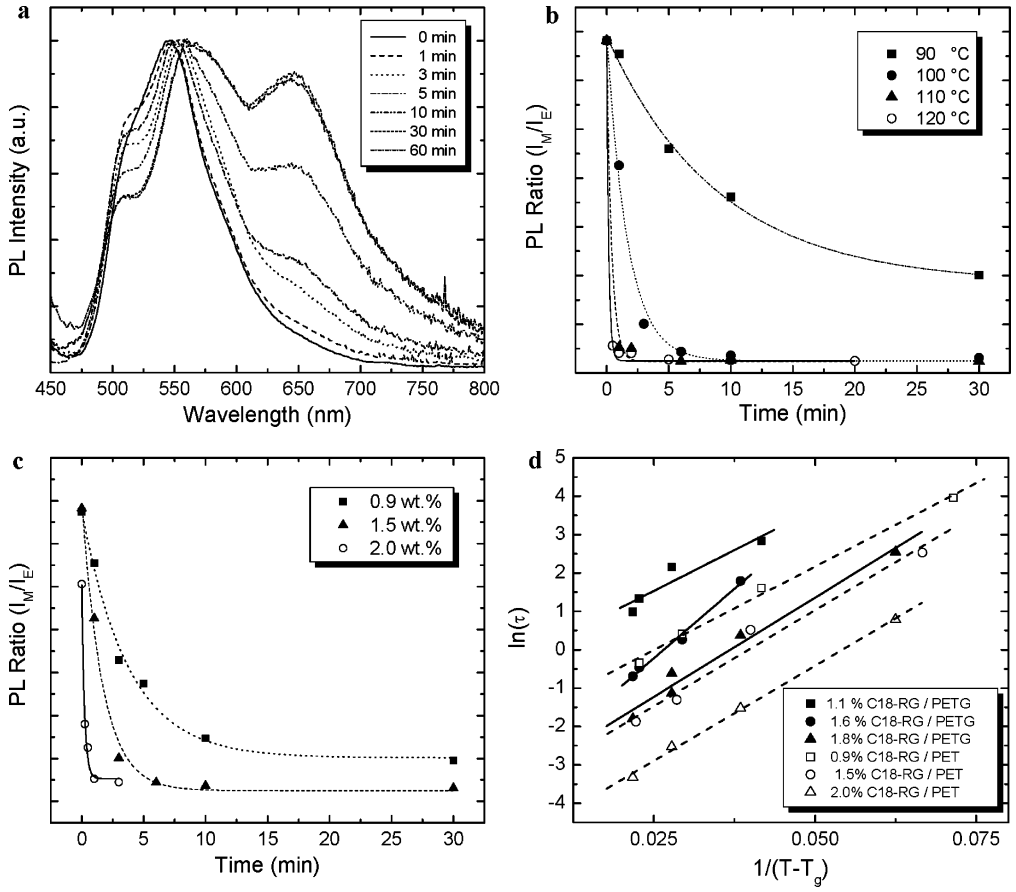


**Figure 5.** (a) PL emission spectra of an initially quenched blend film of PET and 0.9% w/w **C18-RG** as a function of annealing time at 100 °C. (b) Relative intensities of monomer to excimer emission $I_M/I_E$ extracted from the spectra shown in (a) as a function of time (filled circles). Also shown are data obtained in a similar manner at 90 °C (filled squares), 110 °C (filled triangles), and 120 °C (empty circles). (c) Relative intensities of monomer to excimer emission $I_M/I_E$ as a function of annealing time at 100 °C. Shown are data for initially quenched PET/**C18-RG** blends comprising 0.9% w/w (filled squares), 1.5% w/w (filled triangles), and 2% w/w (empty circles) of the dye. Lines represent least-squares fits according to eq 1. (d) Plot of the natural logarithm of the aggregation rate constants $\tau$ (obtained by fitting the data shown in (b) and (c) to eq 1) against $1/(T - T_g)$. Shown are data for blends of PET and between 0.9 and 2% w/w **C18-RG** or blends of PETG and between 1.1 and 1.8% w/w **C18-RG**.

annealed for different times at 100 °C and shows that the relative contributions of monomer ($I_M$, measured at 546 nm) and excimer ($I_E$, measured at 637 nm) emission change gradually as a function of time. The ratios $I_M/I_E$ extracted from these spectra and similar data sets acquired at different annealing temperatures between 90 and 120 °C are plotted as a function of annealing time in Figure 5b. The data of comparative aggregation experiments that were conducted at the same temperature (100 °C) but with blends comprising 0.9, 1.5, or 2% w/w of the dye are shown in Figure 5c. As can be seen from Figures 5b and 5c, for any given temperature and concentration the kinetic data are well-described by a single-exponential function

$$I_M/I_E = I_{M\infty}/I_{E\infty} + Ae^{-t/\tau} \quad (1)$$

where $I_{M\infty}/I_{E\infty}$ is the ratio of the intensities of monomer and excimer emission after annealing to equilibrium, $t$ is the

annealing time, and $A$ and $\tau$ are constants representing the magnitude of change in $I_M/I_E$ and the rate of the change. Figure 5c reveals that for a given temperature the aggregation rate constant $\tau$ decreases significantly with dye concentration, and the process appears to be well-described by Johnson−Mehl−Avrami−Kolmogorov transformation kinetics.[28] As is evident from Figure 5d, ln $\tau$ scales linearly with $1/T$ or $1/(T - T_g)$, indicating that for a given system widely used phenomenological descriptions for the viscoelastic behavior of glassy materials above $T_g$,[29] such as the Vogel−Fulcher−Tamann−Hesse equation,[30] the Williams−Landel−Ferry equation,[31] or the Doolittle equation[32] might be used to express the aggregation kinetics of the cyano-OPV sensor molecules by way of time−temperature superposition. Thus, the aggregation process in the semicrystalline PET/dye blends investigated here appears to be predictable, and for a given composition the fluorescence color of the sample is characteristic of its thermal history. We should highlight the fact that PET and other semicrystalline materials that may be used as matrix for such indicators are not tacky when heated above $T_g$, which represents a significant technological advantage over the hitherto used glassy amorphous systems.[15]

Figure 4 reveals another feature of the annealing process that needs to be discussed, namely, that the different annealing protocols lead not only to different fluorescence colors but also to different degrees of opacity. A comparison of, for example, samples annealed for 10 min at 90 °C and for 30 s at 140 °C makes this aspect evident. This effect is related to crystallization of the host polymer, which also occurs during annealing. To explore if the processes of dye aggregation and crystallization of the host polymer could be separated, we probed the relation between the annealing protocol, the sample's crystallinity, and its PL characteristics in detail for blend films of PET and 0.9% w/w **C18-RG**. The absence of a cold crystallization peak in DSC traces of annealed samples (see Supporting Information) reveals that the crystallization of PET is essentially complete in ca. 30 min at 90 °C, 3 min at 100 °C, and 15 s at 120 °C, respectively. A comparison with Figure 4 shows that under none of these conditions has the dye completely aggregated. Thus, it appears that in the present materials crystallization of the PET paves the way for aggregation, presumably by expression of dye from the crystallizing PET, which leads to an increase of the effective dye concentration in the amorphous portion of the host polymer. We should note that, rather interestingly, annealing of the quenched PET/**C18-RG** blend films not only leads to a pronounced change of the materials' emission color but also caused a significant change of their optical absorption characteristics, altering the appearance of the blends under ambient illumination from yellow-green to orange. We are currently further investigating the nature of this effect, which may represent a most attractive alternative means (to fluorescence color change) for signal transduction.

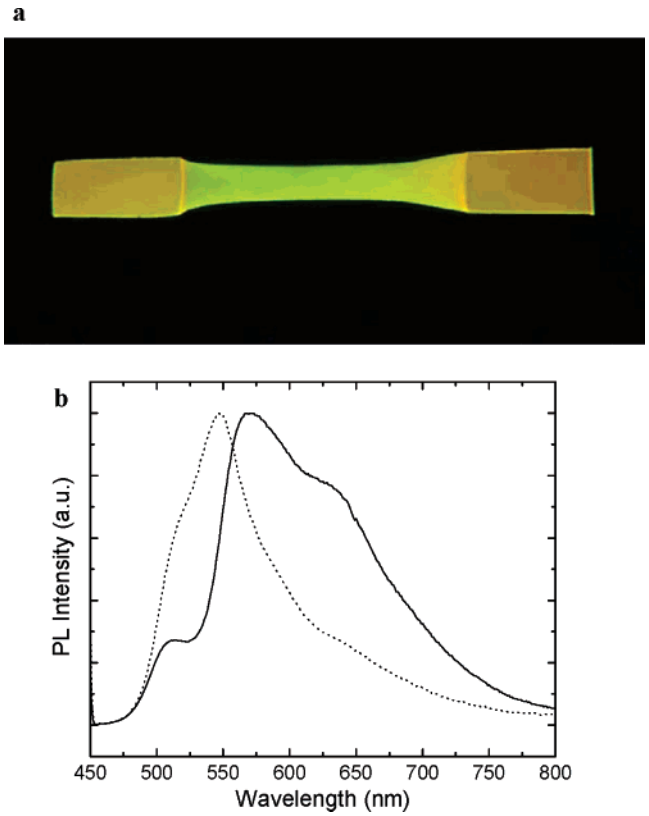


**Figure 6.** Picture (a) and normalized PL emission spectra (b) of a blend film of PET and 0.9% w/w **C18-RG** before (solid) and after (dotted) stretching at room temperature to a draw ratio of 400%. The picture was taken under excitation with UV light of a wavelength of 365 nm. The film had previously been annealed for 15 s at 110 °C.

Finally, we investigated the influence of solid-state tensile deformation on the emission characteristics of 0.9% w/w PET/**C18-RG** films. To exclude temperature effects, tensile deformation experiments were conducted at room temperature. The samples had been annealed before, with the objective of introducing nanoscale dye aggregates which display excimer emission. It should be noted that fully crystallized films were brittle and could not be well-stretched at room temperature. The annealing conditions were therefore chosen to achieve a compromise between drawability and extent of excimer emission. Best color changes upon tensile deformation were observed for films that had been annealed at 110 °C for 15 s. Figure 6a shows that, upon stretching of the films to a draw ratio $\lambda = (l - l_0)/l_0$ of 400%, a significant, irreversible change of the emission color from orange to green can be observed.[33] Concomitantly, PL emission spectra (Figure 6b) show a substantial change from excimer-rich to monomer-dominated emission. These results reflect the transformation of a phase-separated nanocomposite (with presumably very small dye aggregates) into an apparent

(28) (a) Avrami, M. A. *J. Chem. Phys.* **1939**, *7*, 1103. (b) Avrami, M. A. *J. Chem. Phys.* **1940**, *8*, 212. (c) Avrami, M. A. *J. Chem. Phys.* **1941**, *9*, 177. (d) Johnson, W. A.; Mehl, R. F. *Trans. Am. Inst. Mining. Met. Eng.* **1939**, *135*, 416. (e) Ruitenberg, F.; Woldt, E.; Petford-Long, A. K. *Thermochim. Acta* **2001**, *378*, 97.

(29) Ferry, J. D. *Viscoelastic Properties of Polymers*, 3rd ed.; Wiley: New York, 1980.

(30) (a) Vogel, H. *Phys. Z.* **1921**, *22*, 645. (b) Fulcher, G. S. *J. Am. Ceram. Soc.* **1925**, *8*, 339. (c) Tammann, G.; Hesse, W. *Z. Anorg. Allg. Chem.* **1926**, *156*, 245.

(31) Williams, M. L.; Landel, R. F.; Ferry, J. D. *J. Am. Chem. Soc.* **1955**, *77*, 3701.

(32) Doolittle, A. K. *J. Appl. Phys.* **1951**, *22*, 1471.

(33) Annealing above $T_g$ led to reaggregation of the dye molecules; we observed that the relative contribution of excimer emission was significantly higher in the unstretched than in the stretched portions of the film.

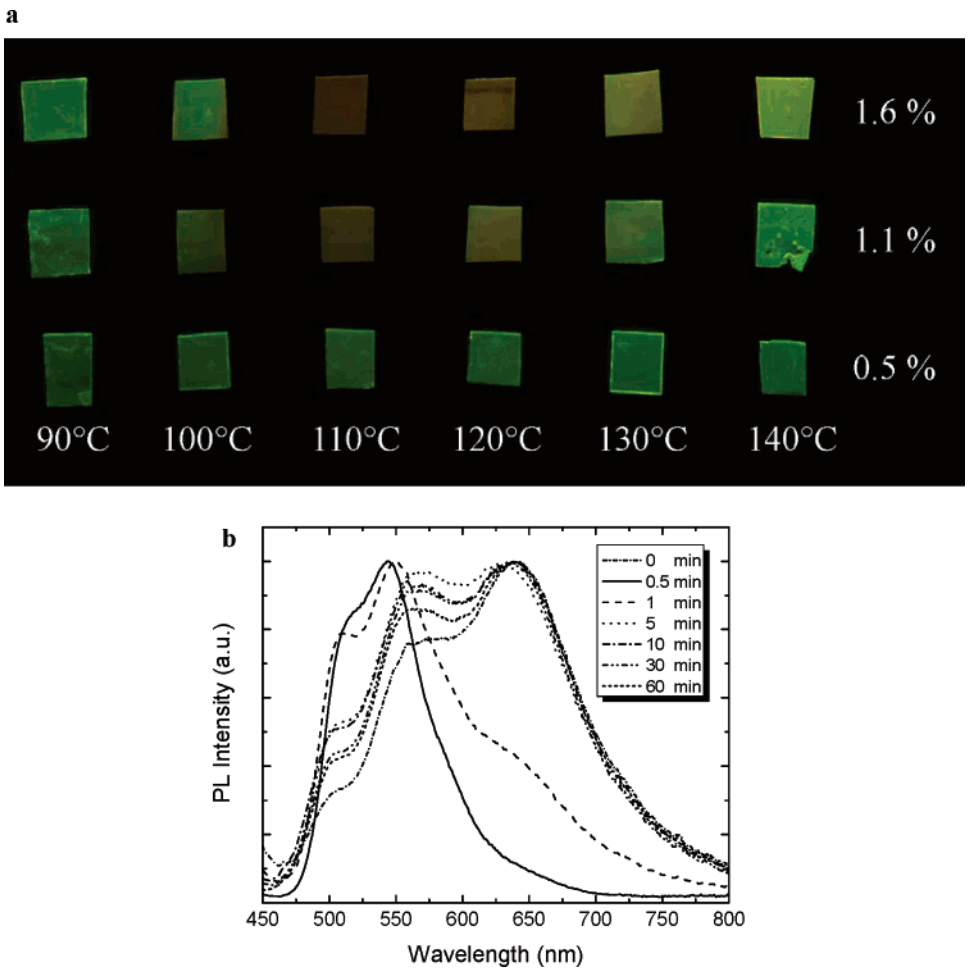


**Figure 7.** (a) Pictures of initially quenched blend films of PETG and different concentrations of **C18-RG.** The samples were annealed for 3 h at the temperature indicated and are shown under illumination with UV light of a wavelength of 365 nm. (b) Normalized PL emission spectra of an initially quenched blend film of PETG and 1.8% w/w **C18-RG** as a function of annealing time at 110 °C.

molecular dispersion or solution upon deformation and confirm that molecular-level shear-induced mixing is possible in a ductile, semicrystalline polymer deformed below their glass transition temperature.

**Blends of Sensor Dyes with PETG.** Primarily to investigate if the deformation sensing scheme would also be applicable to ductile amorphous polymers, and taking advantage of the possibility to compare these materials with the PET-based blends discussed above, we also investigated a blend of poly(ethylene terephthalate glycol) (an amorphous PET with a $T_g$ at 78 °C, obtained by introduction of 1,4-cylclohexylene-dimethylene terephthalate as a comonomer) and between 0.5 and 1.8% w/w **C18-RG**. These blends were prepared by the same melt-processing protocol used for the PET blends, but a slightly lower processing temperature (250 °C) was chosen. Quenched PETG blend films comprising **C18-RG** at all concentrations investigated here display PL emission spectra that are virtually identical to those of quenched PET/**C18-RG** films, featuring a green monomer fluorescence band ($\lambda_{max} \approx 544$ nm) that reflects the molecularly dispersed nature of the dye in the PETG matrix. DSC traces of blends containing **C18-RG** (Supporting Information) reveal slight reductions in the $T_g$ to 76, 74, and 74 °C for blends comprising 1.1, 1.6, and 1.8% w/w of the dye, respectively. In addition, the DSC traces of the blends further display an exothermic signal around 110 °C and a broad endothermic transition around 140 °C, which we assign to phase separation/crystallization of the dye and melting/dissolution of the dye, respectively. The absence of any transitions above 145 °C suggests that, under the processing conditions chosen, the dye is completely dissolved in the polymer host.

To compare the aggregation process of the PETG/dye blends with those of the PET-based materials, we conducted annealing experiments with PETG blends in the temperature range from 90 to 140 °C. A picture of a series of blends films containing between 0.5 and 1.6% **C18-RG** that were annealed for 3 h gives a good visual summary of the kinetics and thermodynamics of excimer formation (Figure 7). As expected, an increase of the dye concentration leads to an increase of orange excimer emission in the annealed films. Samples comprising 0.5% w/w of the dye show green monomer emission under all annealing conditions, while the 1.1% blends displayed an orange hue upon annealing at 110 °C, suggesting that the solubility of **C18-RG** in PETG at this temperature is between ca. 0.5 and 1% w/w. Not surprisingly, the 1.6% w/w PETG/**C18-RG** blends show the most pronounced optical changes of the series shown. For this system the contribution of excimer emission is most pronounced at ca. 110 °C and decreases at higher temperatures to almost vanish at 140 °C. These data suggest that, for the empirically chosen annealing time of this experiment

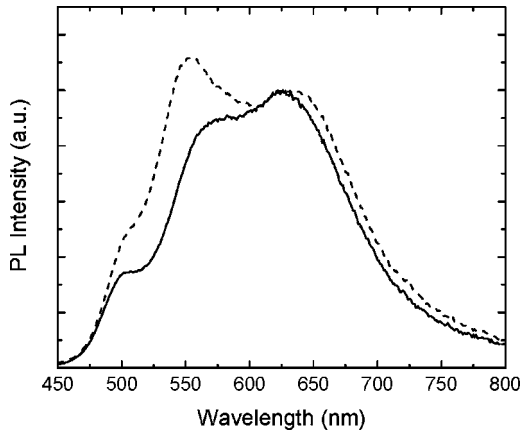


**Figure 8.** Normalized PL emission spectra of a blend film of PETG and 2% w/w **C18-RG** before (solid) and after (dotted) stretching at room temperature to a draw ratio of 400%. The film had previously been annealed for 10 min at 110 °C.

(3 h), the emission characteristics of this blend are governed by kinetic effects below 110 °C (slow aggregation), while the thermodynamic equilibrium dictates molecularly mixed systems at temperatures above ca. 140 °C for all the blends shown here. Of course, this temperature can be shifted by increasing the concentration of the dye as demonstrated by a comparison of the blend containing 1.1% w/w **C18-RG**, which is completely dissolved at 140 °C, to the blend containing 1.6% w/w **C18-RG**, which continues to display a small amount of excimer emission at 140 °C.

To probe kinetics of the aggregation process in this system, we again undertook a detailed spectroscopic investigation. Figure 7b displays the spectra of 1.8% w/w PETG/**C18-RG** blend films annealed for different times at 110 °C. The spectra show very similar features as the PET/**C18-RG** blends discussed before and the relative contributions of monomer ($I_M$, measured at 546 nm) and excimer ($I_E$, measured at 650 nm) emission change in an expected manner. $I_M/I_E$ extracted from spectra of annealed films were fitted to eq 1 in the same manner as was done for annealed PET/**C18-RG** blend films and the data are included in Figure 5d, to allow for a direct comparison. It is noted that phase separation occurs somewhat more slowly in PETG than in PET blends of a similar dye concentration, in qualitative agreement with the fact that expression of dye from the crystallizing PET leads to an increase of the effective dye concentration in this system, which as was discussed before accelerates the aggregation process significantly.

Finally, we also investigated the influence of tensile deformation on the emission characteristics of PETG/**C18-RG** blend films. Films based on a 1.8% w/w blend were exposed to a variety of annealing conditions between 90 and 120 °C for between 1 and 120 min and subsequently stretched to a draw ratio of $\lambda = (l - l_0)/l_0 = 400\%$. All films showed similarly modest increases in $I_M/I_E$ upon stretching. This effect is illustrated in Figure 8 using the example of a film that had been annealed at 110 °C for 10 min prior to deformation. Thus, shear-induced mixing appears to be also at play in the case of the fully amorphous PETG/dye blends investigated here. However, the changes observed in this system were much less pronounced than in the case of the semicrystalline PET blends studied here and the polyolefin blends investigated before.[12,13] In view of the fact that crystallinity is the most prominent difference between these host polymers, we speculate that this feature plays an important role by promoting the formation of sufficiently small excimer-forming dye aggregates (which are subject to dispersion upon deformation of the host polymer, very much in contrast to large dye crystals[13]). This supposition is supported by preliminary AFM experiments, which revealed large dye crystals upon annealing of PETG/**C18-RG** blend films. To develop a better understanding of this important aspect, we intend to conduct a more detailed, comparative study directed toward the investigation of aggregate size in the future.

## Conclusions

In summary, we have demonstrated that the phase behavior of binary blends of PET or PETG and cyano-OPVs can be controlled via the nature of (in)solubilizing groups attached to the dye, the dye concentration, the detailed processing conditions, and the thermal history of the material. In particular, the introduction of long aliphatic groups renders the cyano-OPVs sufficiently insoluble in polyesters so that these dyes may be employed as "molecular probes". Homogeneous blends can be produced by conventional melt-processing protocols that are concluded with a quenching step and the materials thus prepared display emission spectra that are characteristic of the dyes' monomer emission. Annealing above the glass transition temperature of the polyester leads to the formation of excimers and causes significant changes of the materials' emission characteristics. The aggregation processes in the semicrystalline PET/dye blends and amorphous PETG/dye blends investigated here appear to be well-described by single-exponential transformation kinetics, and the fluorescence color of the materials is characteristic of their thermal history. Subjecting appropriately processed samples to mechanical deformation can significantly change the extent of molecular aggregation of the photoluminescent guest molecules, which in turn leads to a variation of the contributions of monomer and excimer emission. The stimuli-responsive properties displayed by the materials systems investigated appear to bear significant potential for wide technological application, in particular, the use of such dyes as "built-in" threshold temperature sensors and internal strain sensors and even crystallization detection sensors in conventional thermoplastic polymers such as PET.

**Acknowledgment.** We are indebted to Ms. Jill Kunzelman, Ms. Kara Smith, and Ms. Shan Tie for technical assistance and thank Dr. Robert Simha for stimulating discussions. We gratefully acknowledge financial support from the National Science Foundation (NSF DMI-0428208), DuPont (Young Professor Award to C.W.), and Toyobo.

**Supporting Information Available:** PL emission spectra of $CHCl_3$ solutions of **C12-RG** and **C12-YB**, PL emission spectra of blend films based on PET and 1% w/w **C1-RG**, 0.2% w/w **C18-RG**, and 0.5% w/w **C18-RG**, and DSC traces of annealed PET/**C18-RG** and quenched PETG/**C18-RG** blend films (PDF). This material is available free of charge via the Internet at http://pubs.acs.org.

CM052186C